Available online at www.sciencedirect.com
ScienceDirect
Structural Safety 29 (2007) 146–163
STRUCTURAL SAFETY
www.elsevier.com/locate/strusafe

Probabilistic response evaluation for RC flexural members subjected to blast loadings

Hai-Cheng Rong, Bing Li *

Protective Technology Research Centre, Nanyang Technological University, 50 Nanyang Avenue, Singapore 639798, Singapore

Received 3 March 2006; accepted 6 March 2006
Available online 6 June 2006

Abstract

The probabilistic responses of the maximum displacement and displacement ductility factor for a reinforced concrete (RC) flexural member against potential blast loadings are evaluated through a nonlinear dynamic analysis of its equivalent single-degree-of-freedom (SDOF) system. Monte-Carlo simulation is used in the analysis. Some differences are observed between the actual responses of the RC member and those of the equivalent SDOF system due to the complex behaviours of reinforced concrete structural members under blast conditions. Two non-dimensional indices are defined to quantify the differences and their expressions are generated through a large amount of numerical and statistical analyses. The approach of utilizing the indices into a probabilistic response assessment of RC flexural members accounting for different kinds of uncertainties is illustrated via four numerical examples which are verified through nonlinear dynamic finite element analysis. It is concluded that the probabilistic response of RC flexural members obtained from the developed approach have a similar distribution with those from probabilistic nonlinear finite element analysis.

Keywords: Equivalent SDOF system; Non-dimensional indices; Maximum displacement; Displacement ductility factor; Monte-Carlo simulation

1. Introduction and background

Information on the probabilistic responses of the maximum displacement and displacement ductility factor is of critical importance for the reliable design or analysis of reinforced concrete (RC) flexural members that might be affected by blast loadings [1–3]. The probabilistic analysis based on a combination of nonlinear dynamic finite element analysis of structural members under blast conditions and Monte-Carlo simulation is computationally considerably more expensive due to the significant geometric and material nonlinearity of RC members [4–6]. Therefore, a simple and efficient way for probabilistic evaluation of the blast responses for RC members is necessary.

* Corresponding author. Tel.: +65 67905316; fax: +65 67910676.
E-mail address: cbli@ntu.edu.sg (B. Li).

0167-4730/$ - see front matter
doi:10.1016/j.strusafe.2006.03.004

Nomenclature

d	effective depth of the RC member measured from the extreme compression fiber to the centroid tensile reinforcement
E_{dc}	dynamic Young's modulus of elasticity for concrete
E_{ds}	dynamic Young's modulus of elasticity for steel
E_{e_y}, E_{e_μ}	mean values of e_y and e_μ, respectively
e_y, e_μ	nominal random variables
F	blast load from idealized triangular pulse
f_{dc}	strength of concrete in compression in dynamic conditions
f_{dv}	dynamic stirrup yield strength
f_{ds}	strength of flexural steel in dynamic conditions
i	impulse
K_{LE}, K_{ME}	transformation load and mass factor, respectively
l	length of the member
P_r	pressure
R	standoff distance
t_d	load duration
W	explosive charge mass expressed in kg of TNT
y_e^{eq}	elastic displacement response of the equivalent SDOF system of the designed RC member due to blast loading
y_e^{rc}	elastic displacement response of the designed RC member at the significant point due to blast loading
y_m^{eq}	maximum displacement response of the equivalent SDOF system of the designed RC member due to blast loading
y_m^{rc}	maximum displacement response of the designed RC member at the significant point due to blast loading
y_t	target displacement
ζ_y^{rc}	non-dimensional displacement index
ζ_μ^{rc}	non-dimensional displacement ductility index
μ^{eq}	displacement ductility response of the equivalent SDOF system of the designed RC member under the given blast loading
μ^{rc}	displacement ductility response of the designed RC member at the significant point due to blast loading
μ_t	target displacement ductility ratio
ρ	longitudinal tension reinforcement ratio
σ_{e_y}, σ_{e_μ}	standard deviations

The maximum displacement and displacement ductility responses of RC flexural members under blast loadings that are simplified into triangular pulses can be determined in an approximate way by transforming the continuous members into equivalent single-degree-of-freedom (SDOF) systems by taking these responses of equivalent systems to be equal to those of the members [7]. However, considering the complicated material behaviours of the concrete and reinforcement under blast conditions, some differences do exist between the actual responses (y_m^{rc} and μ^{rc}) of a RC structural member and those (y_m^{eq} and μ^{eq}) of the equivalent SDOF system as indicated in Fig. 1. But if the indices quantifying the above differences can be obtained, they will provide a simpler way to the estimation of the deformation response of the RC flexural member under the blast conditions from those of the equivalent SDOF system and without performing nonlinear finite element analysis.

This paper aims to present a simple approach for the development of response surfaces for y_m^{rc} and μ^{rc} of RC flexural members against blast loadings. For this purpose, the distribution of two non-dimensional indices quantifying the differences between the responses of RC members and those of equivalent SDOF systems are

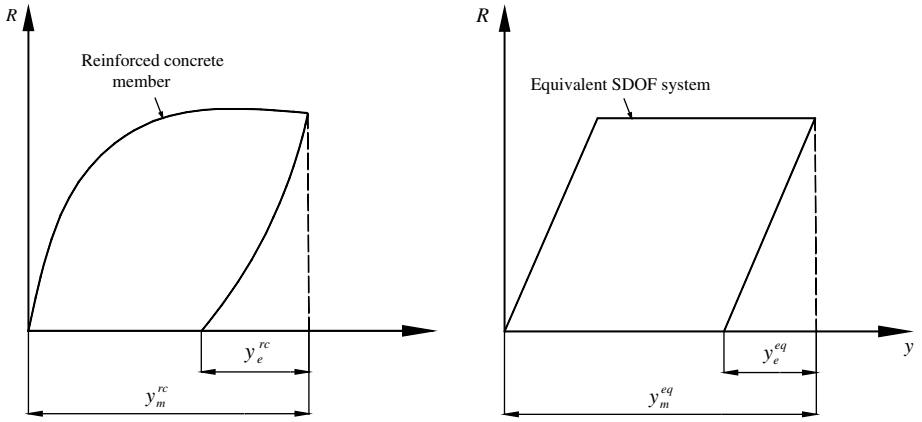

Fig. 1. Response differences between the RC flexural member and the equivalent SDOF system (where $\mu^{rc} = y_m^{rc}/y_e^{rc}$ and $\mu^{eq} = y_m^{eq}/y_e^{eq}$).

firstly derived through extensive numerical studies and fitting. The utilization of these two indices for the probabilistic response assessment of y_m^{rc} and μ^{rc} is further addressed by the combination of the Monte-Carlo simulation. As an illustration, the blast responses of four flexural members with different kinds of support conditions are probabilistically evaluated and numerically verified by comparing the results with those from probabilistically nonlinear finite element analysis.

2. Response differences between RC flexural members and equivalent SDOF systems

2.1. Definition of the non-dimensional indices quantifying the differences

To obtain a consistent measurement of the degree of the differences between the actual responses (y_m^{rc} and μ^{rc}) for the flexural member under a certain blast loading and the their respective equivalent SDOF system (y_m^{eq} and μ^{eq}), two non-dimensional indices are defined as

$$\varsigma_y^{rc} = \frac{y_m^{eq} - y_m^{rc}}{y_m^{eq}} \tag{1}$$

$$\varsigma_\mu^{rc} = \frac{\mu^{eq} - \mu^{rc}}{\mu^{eq}} \tag{2}$$

where ς_y^{rc} is the non-dimensional displacement index standing for the difference between y_m^{rc} and y_m^{eq}; ς_μ^{rc} is the non-dimensional displacement ductility index representing the difference between μ^{rc} and μ^{eq}. Eqs. (1) and (2) describe the basic relationships between (y_m^{rc}, μ^{rc}), (y_m^{eq}, μ^{eq}) and $(\varsigma_y^{rc}, \varsigma_\mu^{rc})$. With ς_y^{rc} and ς_μ^{rc} initially known, values of y_m^{rc} and μ^{rc} can be obtained from y_m^{eq} and μ^{eq}. However, depending on these two equations to estimate ς_y^{rc} and ς_μ^{rc} seems to have few advantages since y_m^{rc} and μ^{rc} have to be firstly computed. This entails explosion testing or numerical finite element analysis of the RC members under blast conditions, which would be sure to be costly or involve intensive computational effort. Therefore, simple alternative formulae for the determination of ς_y^{rc} and ς_μ^{rc} rather than Eqs. (1) and (2) need to be developed.

2.2. Symbolical expressions of the non-dimensional indices

By controlling the responses of the equivalent SDOF system (y_m^{eq} and μ^{eq}) to be exactly equal to their respective design performance targets (y_t and μ_t), the design solution of effective depth (d) and longitudinal reinforcement ratio (ρ) for a RC flexural member can be specifically gained with the given basic variables including the peak reflected pressure (P_r) and duration of blast loadings (t_d), the support condition, the length (l) and the properties of concrete and reinforcement under the dynamic conditions (f_{dc}, E_c, f_{ds}, E_d, and f_{dv}) [13]. Accordingly, the actual responses (y_m^{rc} and μ^{rc}) of the specifically designed member under the given blast loading can be specifically determined with the nonlinear finite element analysis. Considering the complicated

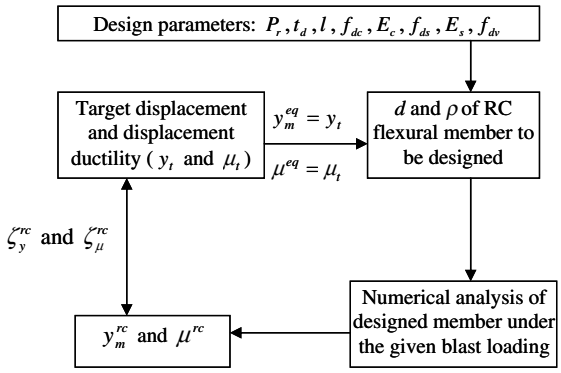

Fig. 2. The procedure to find ς_y^{rc} and ς_μ^{rc}.

behaviours of a RC member under the blast condition, some discrepancies occur between the actual responses (y_m^{rc} and μ^{rc}) and the design performance targets (y_t and μ_t), which also represent the differences between the responses of the designed RC member and those of the equivalent SDOF system as shown in Fig. 2. The responses (y_m^{rc} and μ^{rc}) of the designed member can be determined and then substituted into Eqs. (1) and (2), respectively, to produce ς_y^{rc} and ς_μ^{rc} to be the symbolical functions of these variables as

$$\varsigma_y^{rc} = \varsigma_y^{rc}(P_r, t_d, y_t, \mu_t, l, SC, f_{dc}, E_c, f_{ds}, E_s, f_{dv}, d, \rho) \tag{3}$$

$$\varsigma_\mu^{rc} = \varsigma_\mu^{rc}(P_r, t_d, y_t, \mu_t, l, SC, f_{dc}, E_c, f_{ds}, E_s, f_{dv}, d, \rho) \tag{4}$$

2.3. Analytical procedures

Establishing the explicit expressions of Eqs. (3) and (4) is almost impractical since RC members will exhibit a significantly complicated geometric and material nonlinearity under most blast conditions. A curve fitting technique with a large amount of reliable data for ς_y^{rc} and ς_μ^{rc}, which are determined according to Eqs. (1) and (2) with y_m^{rc} and μ^{rc} obtained from nonlinear dynamic finite element analyses of the designed members, is executed together with the statistical analyses so as to find the simplified explicit expressions of Eqs. (3) and (4). The procedure is listed as follows:

(1) Select the type of support conditions for the RC members to be designed.
(2) Sample the design variable vector of $\{P_r, t_d, y_t, \mu_t, l, f_{dc}, E_c, f_{ds}, E_s, f_{dv}\}'$, where 2000 samples are randomly taken to ensure the accuracy of the statistical analysis.
(3) Design the member with each sample of the design variable vector to obtain d, ρ and further ρ', ρ_v and b_w of a ratio of d.
(4) Repeat step (3) until 2000 sampled design cases are accomplished.
(5) Select 500 design cases with ρ ranging from 0.31% to 2.2%.
(6) Perform numerical analysis on the selected 500 design cases to find y_m^{rc} and μ^{rc} with ABAQUS [18].
(7) Compute ς_y^{rc} and ς_μ^{rc} of the 500 design cases with Eqs. (1) and (2).
(8) Plot the distributions of ς_y^{rc} and ς_μ^{rc} versus these basic design variables.
(9) Carry out the curve fitting of the distributions of ς_y^{rc} and ς_μ^{rc} followed by statistical analyses.
(10) Recommend the simplified formulae to estimate ς_y^{rc} and ς_μ^{rc}.
(11) Change the type of *SC*s of the members and repeat the above steps.

2.3.1. Random selection of basic variables

In order to perform the curve fitting of the distributions of ς_y^{rc} and ς_μ^{rc} to find their simplified formulae, the design variables involved in the second step of the above procedure are randomly sampled within their concerned ranges and is discussed as follows.

The blast loadings that can be reasonably idealized into triangular pulses are basically dependent on the explosive mass expressed in kg of TNT (W) and the standoff distance (R) for external explosions [9,10]. Therefore, the random selections of W and R rather than P_r and t_d is executed in their respective ranges from 50 kg to 1000 kg equivalent TNT and from 4 m to 15 m standoff distance for the blast resistant design in the following analysis. This provides a significantly wide range of blast incidents from the most severe loadings produced by 1000 kg TNT at 4 m distance (a scaled distance $Z = 0.4\ \mathrm{m/kg^{1/3}}$) to the slightest loadings by 50 kg TNT at 15 m distance ($Z = 4.1\ \mathrm{m/kg^{1/3}}$). For the more severe blast situations, the design of the structural system with the alternate load path in redistributing loadings seems to be more reasonable and economic. In this case the structural members immediately opposite the blast are allowed to fail, while in the situations of the lighter blasts, the blast loadings become less critical in the structural design. From W and R, the blast loadings of reflected pressure (P_r) and impulse (i) can be obtained with CONWEP [9] which has been developed based on TM5-855-1 [10] and generally used in the blast-resistant design, while the loadings durations (t_d) are approximately obtained with $2i/P_r$.

The determination of the reasonable design targets of y_t and μ_t should account for possible blast intensities within the blast resistant design of a particular RC member. Hence, the random selection of design targets (y_t and μ_t) is executed in their different ranges according to the various scopes of the blast impulses as shown in Table 1. Some overlaps are allowed for the ranges of y_t and μ_t considering that there is no strict watershed for them at a particular impulse within the design. The maximum allowable y_t and μ_t are taken, respectively, to be larger than the limit of 4° for non-laced RC members as recommended in current design guidance [1–3,10–12]. This is to cover the possibility of the actual responses of the designed members in blast conditions being located on the conservative side when compared with their respective performance targets of y_t and μ_t.

The parameter of l is selected in a range from 4.5 m to 9.0 m for the RC members with two ends constrained while from 2.5 m to 4.5 m for members with one end free, thus covering the most typical cases for RC structures. Due to strain rate effects, the parameters of material properties of concrete and reinforcement under the dynamic conditions are implemented with the possible ranges listed in Table 2. Since the structural members exist in the context of structural systems, their real support conditions are complex and generally depend on the connection with the adjacent members as well as the construction requirements. However, in the blast resistant design they are generally idealized into one of the four types as listed in Table 3. Considering that RC members should be designed to resist the negative deflection or rebound of the members subsequent to its maximum positive deflection and that the possibility of the explosion occurring in the two opposite sides of the members to be designed, the area of compression reinforcement employed is equal to that of the tensile reinforcement area.

Based on the ranges of the variables discussed above, their random samplings are executed by assuming them equally frequent or equally likely to occur. This ensures the likehood of a more general curve fitting of ς_y^{rc} and ς_μ^{rc} which can incorporate the effects of these variables as adequately as possible.

Table 1
Various design targets

Impulse (kPa ms)	$\leqslant 10^3$	10^3–10^4	10^4–2×10^4	2×10^4–3×10^4	$\geqslant 3\times10^4$
θ_t (°)	1–1.8	1.4–3.2	2.8–3.6	3.2–4.0	3.4–4.8
μ_t	3.0–8.5	4.5–10.5	5.5–12.5	6.0–14.5	7.0–16.5

*$y_t = l\tan(\theta_t)/2$ for the member with two ends constrained.
*$y_t = l\tan(\theta_t)$ for member with one end free.

Table 2
Various material properties

Variable	Range
f_c* (MPa)	30.0–40.0
E_c (GPa)	25.5–30.5
f_s** (MPa)	460.0–560.0
E_s (GPa)	190.0–210.0
f_v** (MPa)	250.0–300.0

* $f_{dc} = 1.19\times f_c$.
** $f_{ds} = 1.17\times f_s$, $f_{dv} = 1.17\times f_v$.

Table 3
Various support conditions

Type	Support Condition
Simply-supported	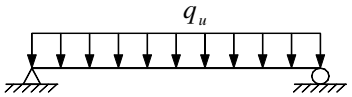
Fixed/free	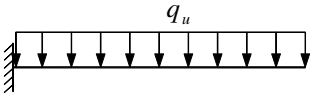
Fixed/roller-supported	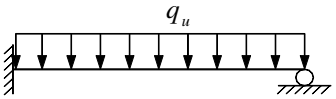
Fixed/fixed	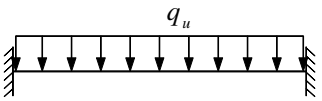

2.3.2. Nonlinear finite element models

The sixth step of the above analytical procedure (the numerical analysis on the designed members to find y_m^{rc} and μ^{rc}) is executed with the program ABAQUS [18]. The failure of RC members under blast conditions is characterized by concrete crushing accompanied by concrete cracking, thus the smeared cracking model for concrete is utilized. In this model, cracking appears when the maximum principal tensile stresses reach a failure surface. To simulate the softening effect of the concrete in tension, a bilinear tension stress–strain curve is used after cracking as shown in Fig. 3, where the failure strain ε_u^{cr} is taken as 10^{-3}. The selection of this value is based on the assumption that the strain softening after failure reduces the stress linearly to zero at a total strain of about 10 times the strain at failure of concrete in tension, which is typically 10^{-4} in the standard concretes [8]. The tensile strength f_t is determined from the compressive strength f_c as [19]

$$f_t = 0.30 f_c^{2/3} \tag{5}$$

In the case of concrete in compression, concrete is simulated with an elastic–plastic mode and the elastic stress state is limited by a yield surface. Once yielding had occurred, an associated flow rule with isotropic hardening is used. The yield surface is determined in terms of the first two stress invariants

$$f = q - \sqrt{3}a_0 p - \sqrt{3}\sigma_c(\varepsilon_{uniaxial}^{pl}) \tag{6}$$

where p is the effective pressure, q is Mises equivalent deviatoric stress, and a_0 is a constant, which is chosen from the ratio of the ultimate stress reached in biaxial compression to the ultimate stress reached in uniaxial compression. $\sigma_c(\varepsilon_{uniaxial}^{pl})$ is the hardening (and softening) parameter that is defined from the uniaxial compression data of the concrete as a function of the plastic strain [19]. The stiffness used in the analysis for unloaded concrete in tension and compression is also given in Fig. 3. When the cracked concrete is unloaded, the secant unloading modulus is utilized as stiffness so that the strain across the crack is reduced linearly to zero as the stress approaches zero. If the load is removed at some point after inelastic straining has occurred for the concrete in compression, the unloading response is softer than that of the initial elastic response, but this effect is ignored in this model. Thus initial elastic stiffness is used when the concrete in compression is unloaded.

The Von-Mises yield criterion is used to describe the constitutive behaviour of the reinforcement. The stress and strain relationship of reinforcement is shown in Fig. 3, where the reinforcement is modelled with an elasto-plastic curve. The strain hardening of reinforcement is not considered in this analysis since it is hard to define under the blast conditions due to a lack of sufficient experimental data plus the ultimate strain value is often not reported in the current literatures due to the difficulty of determining exactly when the peak stress occurs as well as the confusion between ultimate strain and rupture strain.

Considering that both the concrete and reinforcement exhibit increased strengths under higher loading rates, the expressions of dynamic increase factors (DIFs) by Malvar and Crawford [20,21] are adopted. These

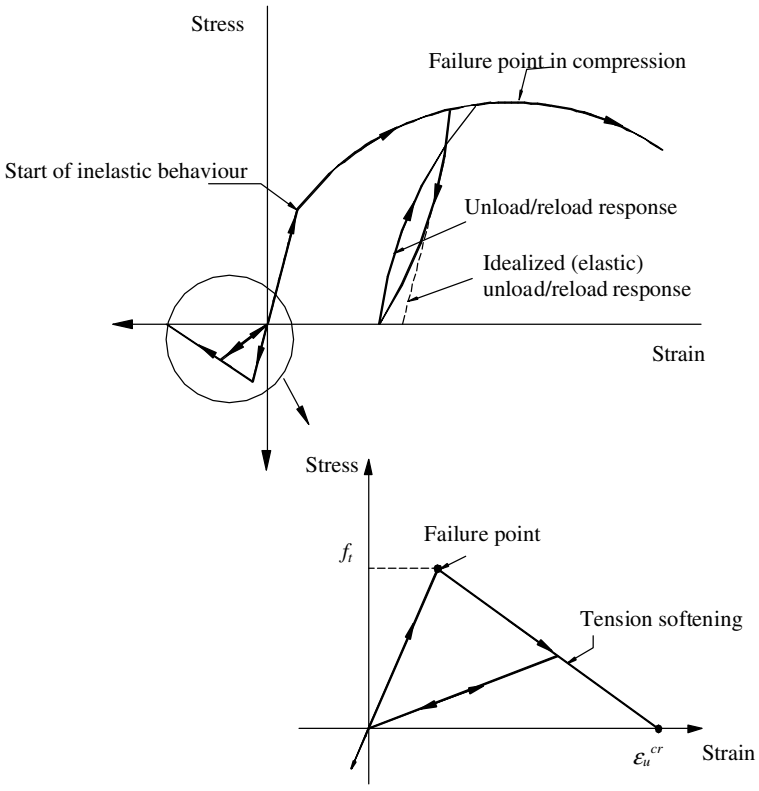

(a) Concrete in compression and tension

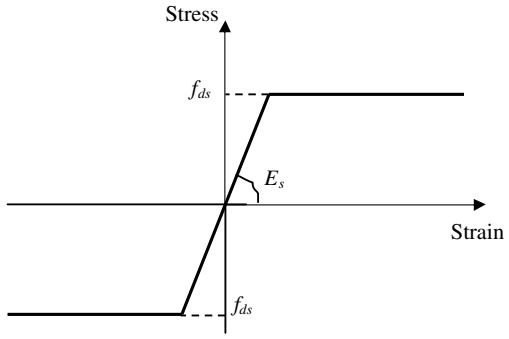

(b) Reinforcement

Fig. 3. Material modelling.

expressions are derived from the literature review of the extensive test data concerning the effects of strain rate on the strength of concrete and reinforcement. For the concrete compressive strength, DIF is given as

$$\mathrm{DIF} = \begin{cases} (\dot{\varepsilon}/\dot{\varepsilon}_s)^{1.026\alpha_s}, & \dot{\varepsilon} \leqslant 30\ \mathrm{s}^{-1} \\ \gamma_s(\dot{\varepsilon}/\dot{\varepsilon}_s)^{1/3}, & \dot{\varepsilon} > 30\ \mathrm{s}^{-1} \end{cases} \tag{7}$$

where $\dot{\varepsilon}$ is the strain rate in the range of 30×10^{-6}–$300\ \mathrm{s}^{-1}$; $\dot{\varepsilon}_s = 30 \times 10^{-6}\ \mathrm{s}^{-1}$ (static strain rate); $\log\gamma_s = 6.156\ \alpha_s - 2$; $\alpha_s = 1/(5 + 9\ f_c/f_{co})$; $f_{co} = 10$ MPa; f_c is the static compressive strength of concrete. For the concrete in tension, the formula is:

$$\mathrm{DIF} = \begin{cases} (\dot{\varepsilon}/\dot{\varepsilon}_s)^{\delta}, & \dot{\varepsilon} \leqslant 1.0\ \mathrm{s}^{-1} \\ \beta(\dot{\varepsilon}/\dot{\varepsilon}_s)^{1/3}, & \dot{\varepsilon} > 1.0\ \mathrm{s}^{-1} \end{cases} \tag{8}$$

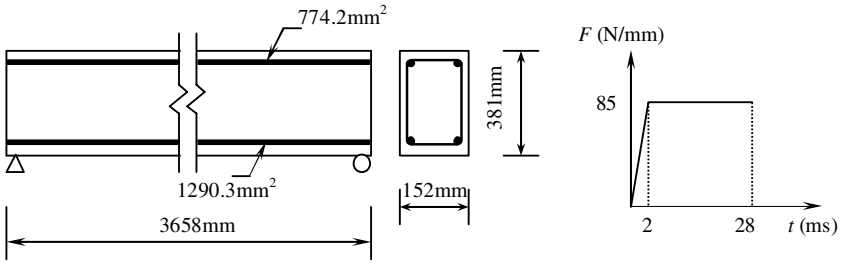

Fig. 4. The details of the simply-supported beam tested by Seabold [22].

where $\dot{\varepsilon}$ is the strain rate in the range of 10^{-6}–$160\ s^{-1}$; $\dot{\varepsilon}_s = 10^{-6}\ s^{-1}$; $\log\beta = 6\delta - 2$; $\delta = 1/(1 + 8\ f_c/f_{co})$; $f_{co} = 10$ MPa. The DIF formula for the yield stress of reinforcement is:

$$\mathrm{DIF} = (\dot{\varepsilon}/10^{-4})^{\alpha} \tag{9}$$

where $\alpha = \alpha_{fs}$ and $\alpha_{fs} = 0.074 - 0.04 f_s/414$. This formula is valid for reinforcement with yield stresses between 290 and 710 MPa and for strain rates between 10^{-4} and $225\ s^{-1}$. To integrate Eqs. (7)–(9) into the analysis, the user subroutine USDFLD in ABAQUS is used which allows the user to define the field variable at a material point as a function of any of the available material point quantities. Thus by taking the strain rate as a field variable, the strain rate-dependent material properties can be introduced in the analysis since such properties can be easily defined as functions of strain rate with Eqs. (7)–(9). Timoshenko beam elements are assigned to model the members while the rebar option is utilized to place each reinforcement at its exact location while perfect bond is assumed between the reinforcement and the concrete.

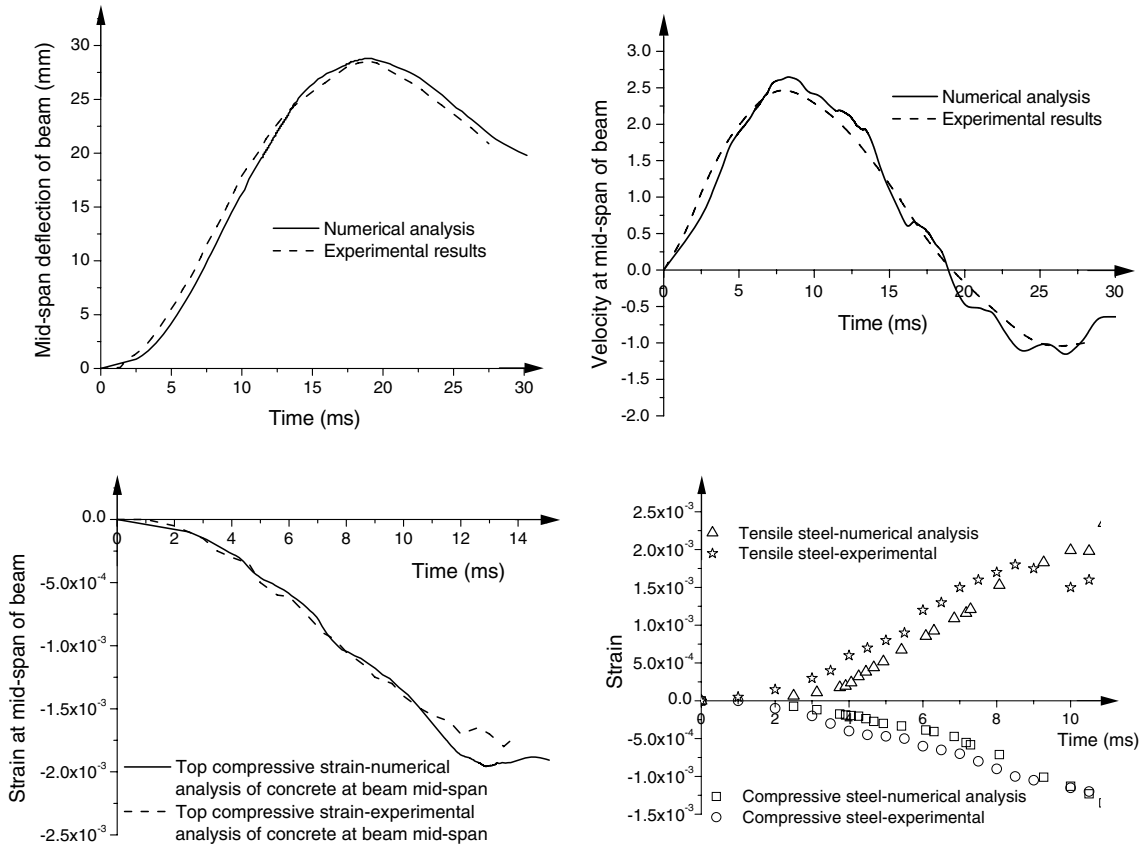

Fig. 5. Verification of finite element models showing comparison between the numerical and experimental results.

The verification of the finite element models as mentioned above is carried out by implementing it into the analysis of a simply supported RC beam subjected to blast loadings tested by Seabold [22] as shown in Fig. 4. The computed and experimental displacement–time history at mid-span is shown for a comparison in Fig. 5. It can be observed that the peak experimental response of 28.5 mm was recorded at the time of 19.5 ms, which closely agreed with the analytical results for which the computed peak displacement of 28.8 mm is reached at the time of 19.2 ms. The recorded permanent deformation of the RC beam was 20.8 mm and it also matched well with the predicted deflection of 21.7 mm. In addition, the analytical and experimental results of the mid-span velocity history, the top compressive strain history of concrete, plus the strain history of the main reinforcement of the beam are also compared in Fig. 5. It is demonstrated that the numerical analysis has a good agreement with the observed experimental behaviours and thus the numerical model has the ability to simulate the failure process of concrete and reinforcement.

2.4. Distributions of the non-dimensional indices

Based on the above analytical procedure, the distributions of $\varsigma_y^{\mathrm{rc}}$ and $\varsigma_\mu^{\mathrm{rc}}$ for the designed RC members versus ρ under various support conditions are obtained in Figs. 6–9. It can be observed that the distributions of $\varsigma_y^{\mathrm{rc}}$ are generally concentrated in the strips that are much narrower and closer to the X-axis as compared to those of $\varsigma_\mu^{\mathrm{rc}}$ especially in the situation of the first three types of support conditions. This indicates that the discrepancies between $y_{\mathrm{m}}^{\mathrm{rc}}$ and $y_{\mathrm{m}}^{\mathrm{eq}}$ are much smaller than those of μ^{rc} with μ^{eq}. This result is reasonable since μ^{rc} is determined by not only $y_{\mathrm{m}}^{\mathrm{rc}}$ but also the elastic displacement of $y_{\mathrm{e}}^{\mathrm{rc}}$ of the member. As a continuous RC member is converted into an equivalent SDOF system with its resistance function simplified by a bilinear curve, the elastic displacement of the member in a blast incident is significantly underestimated, which leads to the relatively large positive values of $\varsigma_\mu^{\mathrm{rc}}$.

The convergent distributions of $\varsigma_y^{\mathrm{rc}}$ and $\varsigma_\mu^{\mathrm{rc}}$ with respect to ρ under any support condition as shown in Figs. 6–9 indicate that the importance of parameter ρ, which can be conceptually accounted for from two aspects. In the calculation of the longitudinal reinforcement ratio (ρ) from the ultimate strength R_{m}, the contribution of concrete to R_{m} is ignored within the design. For the members with a small value of ρ where the concrete becomes predominant in resisting external force, this lack of attention will lead to a significantly conservative design and therefore higher conservative values for $\varsigma_y^{\mathrm{rc}}$ and $\varsigma_\mu^{\mathrm{rc}}$. With an increase in ρ, the contribution of concrete to R_{m} becomes smaller and so does the conservative degree of design. It also agrees quite well with the trend of $\varsigma_\mu^{\mathrm{rc}}$ with respect to ρ under all support conditions and $\varsigma_y^{\mathrm{rc}}$ to ρ under the fourth support conditions. The second reason that makes ρ important to $\varsigma_y^{\mathrm{rc}}$ and $\varsigma_\mu^{\mathrm{rc}}$, is related to the calculation of the stiffness of RC members. The stiffness calculated are influenced by a coefficient determined by ρ from the empirical data fitting curve, applied to obtain the cross-sectional moment of inertia along RC members.

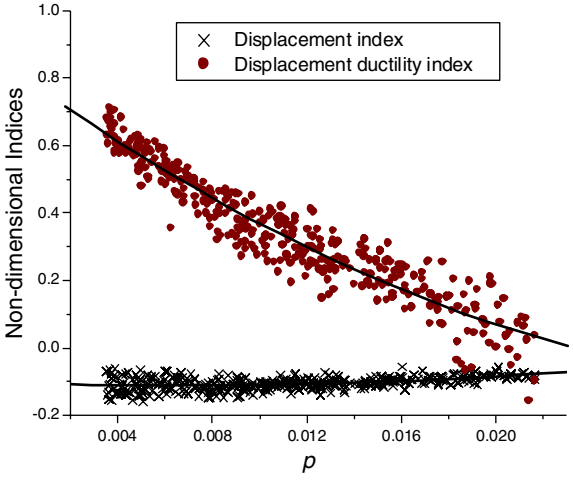

Fig. 6. Distributions of non-dimensional indices with longitudinal reinforcement ratio for simply supported members.

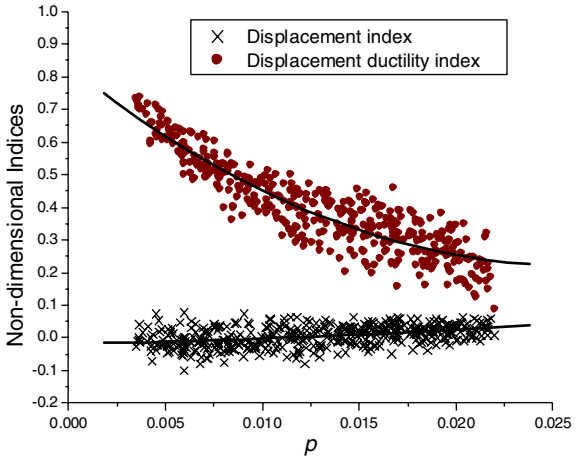

Fig. 7. Distributions of non-dimensional indices with longitudinal reinforcement ratio for fixed/free members.

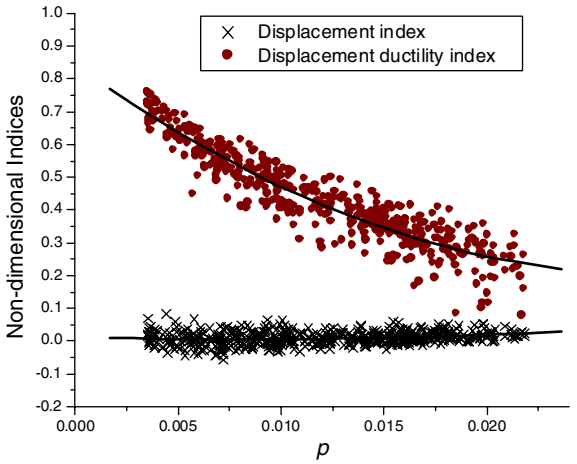

Fig. 8. Distributions of non-dimensional indices with longitudinal reinforcement ratio for fixed/roller-supported members.

The support condition of a structural member also plays an important role in producing ς_y^{rc} and ς_μ^{rc}, which is demonstrated by the trends of ς_y^{rc} and ς_μ^{rc} with ρ under various support conditions. Comparing Figs. 6–8 with Fig. 9 indicates that both ς_y^{rc} and ς_μ^{rc} for fixed/fixed members are generally larger than those of members under other support conditions with the same ρ. This difference is induced by the application of the unreasonable transformation factors K_{LE} and K_{ME} in the design of fixed/fixed members. Fig. 10 shows the transformation of this type of continuous RC member into the equivalent SDOF system can be divided into three stages with different values of transformation factors at each stage: the elastic stage with no plastic hinges, the elastic–plastic stage when two plastic hinges occurs at the two ends of the member and the purely plastic stage where a third plastic hinge appears in the mid-span. In the second stage, transformation factors are taken with the same values as those for a simply supported member. However, the responses of a member with two ends pinned (plastic hinges formed at both ends) will be surely smaller than those of a simply supported member. This means the responses of fixed/fixed members are overestimated during the design thus leading to relatively larger ς_y^{rc} and ς_μ^{rc}.

The variables other than ρ and support conditions have some minor effects, which make the values of ς_y^{rc} and ς_μ^{rc} slightly scattered as ρ and support condition are certain. Although these effects of other variables are not significant, they are also incorporated in the recommended formulae while considering all variable effects.

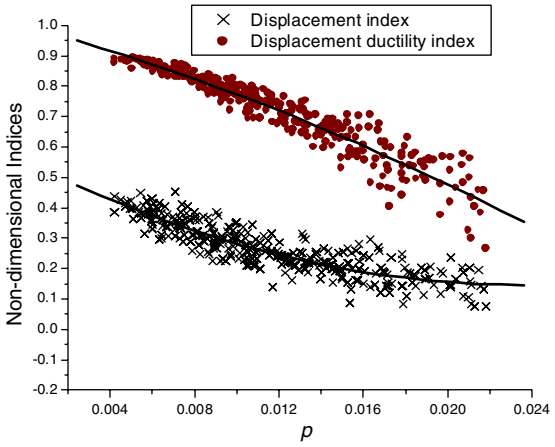

Fig. 9. Distributions of non-dimensional indices with longitudinal reinforcement ratio for fixed/fixed members.

2.5. Formulae for the non-dimensional indices

In order to obtain the simplified expressions of Eqs. (3) and (4), the relevant variables are divided into two groups: the important variables of ρ and support condition, and the secondary variables including P_r, t_d, y_t, μ_t, and d. To incorporate the influences of ρ and support condition into the expressions, the nonlinear curve fittings of ς_y^{rc} and ς_μ^{rc} versus ρ for various support conditions as plotted in Figs. 6–9, are carried out where the functions are expressed as $f(\rho, SC)$ and $g(\rho, SC)$, respectively. The effects of the secondary variables are dealt with by introducing the two nominal random variables of e_y and e_μ that are assumed to represent the deviation of ζ_y^{rc} and ζ_μ^{rc} around the fitting curves. As a consequence, Eqs. (3) and (4) are simplified into

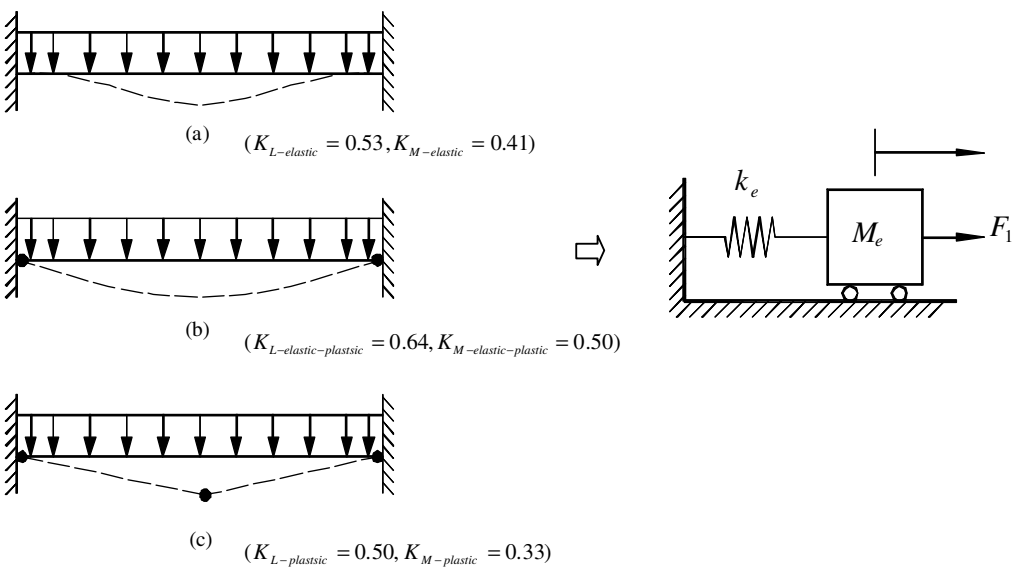

where $K_{ME} = \left((K_{M-elastic} + K_{M-elasto-plastic}) \times 0.5 + K_{M-plastic}\right)/2$, $K_{LE} = \left((K_{L-elastic} + K_{L-elasto-plastic}) \times 0.5 + K_{L-plastic}\right)/2$

$k_e = \alpha \frac{E_c I}{l^3} K_{LE}$, $M_e = K_{ME} \rho_{den} l b_w d$

Fig. 10. Stages of fixed/fixed members in the determination of transformation factors [7,11,12].

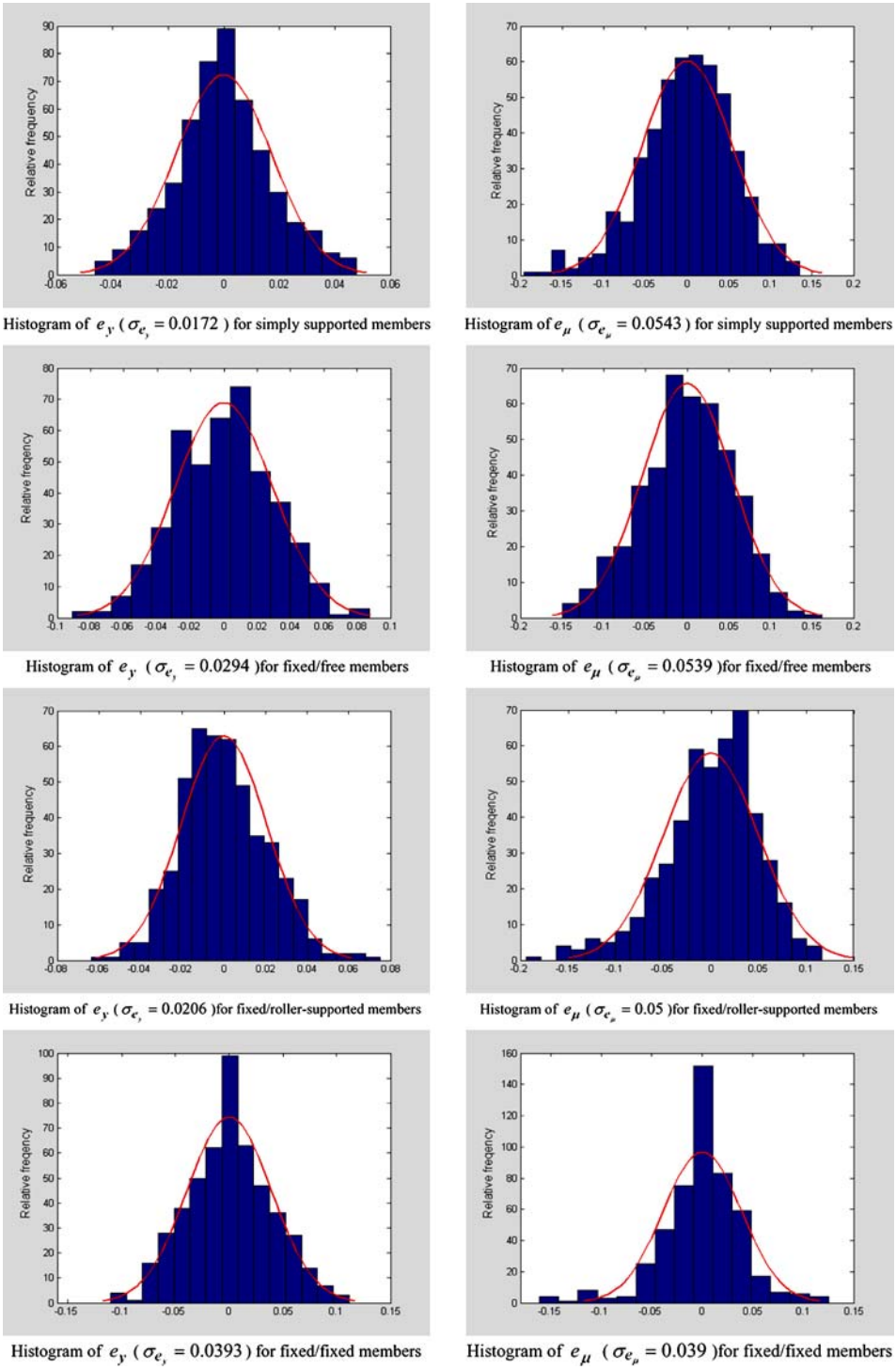

Fig. 11. The distributions of e_y and e_μ for RC members with different support conditions.

$$\varsigma_y^{\mathrm{rc}} = f(\rho, SC) + e_y \tag{10}$$

$$\varsigma_\mu^{\mathrm{rc}} = g(\rho, SC) + e_\mu \tag{11}$$

Table 4
Results of the nonlinear curve fitting

SC	a_1	a_2	a_3
ζ_y^{rc}			
Simply-supported	−0.10369	−2.20114	160.30932
Fixed/free	−0.01712	0.80877	66.84997
Fixed/roller-supported	0.01276	−1.67032	100.93644
Fixed/fixed	0.55459	−34.63653	735.20353
ζ_μ^{rc}			
Simply-supported	0.80257	−50.10919	675.55356
Fixed/free	0.83085	−47.05548	911.90338
Fixed/roller-supported	0.84443	−45.30174	800.57689
Fixed/fixed	0.99826	−18.99113	−354.75711

A quadratic function is selected for the curve fitting given by

$$f(\rho, SC) \quad \text{and} \quad g(\rho, SC) = a_1 + a_2\rho + a_3\rho^2 \tag{12}$$

With the result functions of $f(\rho, SC)$ and $g(\rho, SC)$, the nominal random variables of e_y and e_μ can be obtained with

$$e_y = \zeta_y^{rc} - f(\rho, SC) \tag{13}$$

$$e_\mu = \zeta_\mu^{rc} - g(\rho, SC) \tag{14}$$

For members with various support conditions, the results of the parameters a_1, a_2 and a_3 are listed in Table 4 while the histograms of e_y and e_μ are shown in Fig. 11. It is demonstrated that e_y and e_μ follow normal distribution with the mean values (E_{e_y} and E_{e_μ}) of e_y and e_μ, respectively, approximate to zero. The standard deviations (σ_{e_y} and σ_{e_μ}) of e_y and e_μ, respectively, observed are relatively minor thus indicating the limited effect of the variables other than ρ and support condition.

3. Response evaluation depending on formulae of indices

The importance of applying ζ_y^{rc} and ζ_μ^{rc} is that they provide a simpler way to predicting of the responses (y_m^{rc} andμ^{rc}) for RC flexural member under a possible blast loading without carrying out nonlinear finite element analysis. Substituting Eqs. (10) and (11) into Eqs. (1) and (2), respectively, and rearranging the terms, the response surface of y_m^{rc} and μ^{rc} are obtained as

$$y_m^{rc} = y_m^{eq}(1 - f(\rho, SC) - e_y) \tag{15}$$

$$\mu^{rc} = \mu^{eq}(1 - g(\rho, SC) - e_\mu) \tag{16}$$

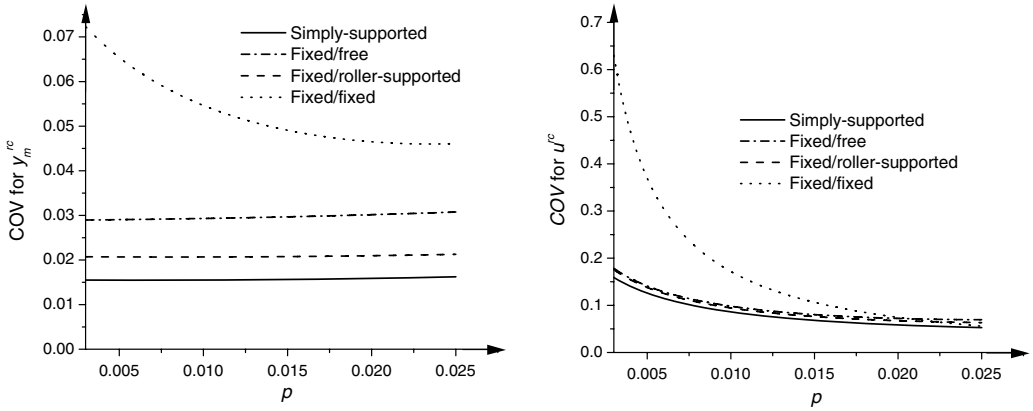

Fig. 12. COVs for y_m^{rc} and μ^{rc} produced by the random effect of e_y and e_μ.

Table 5
Details of four RC flexural members

Example	*SC*	l (m)	d (mm)	$\rho(\rho')$ (%)	f_{dc} (MPa)	f_{ds} (MPa)	E_c (GPa)	E_s (GPa)
I	Simply-supported	5.0	450	0.70	36	520	28	210
II	Fixed/free	4.0	400	1.60	40	506	30	200
III	Fixed/roller-supported	4.5	350	2.00	40	550	30	200
IV	Fixed/fixed	6.0	300	1.00	36	520	28	210

Table 6
Random variables for the members

Variables	Distribution	COV	Lower and upper limit
f_{dc}	Normal	0.08	
f_{ds}		0.08	
E_c		0.15	
E_s		0.15	
A_s		0.05	
d		0.05	
l		0.05	
W	Uniform		50–500 kg
R			5–15 m

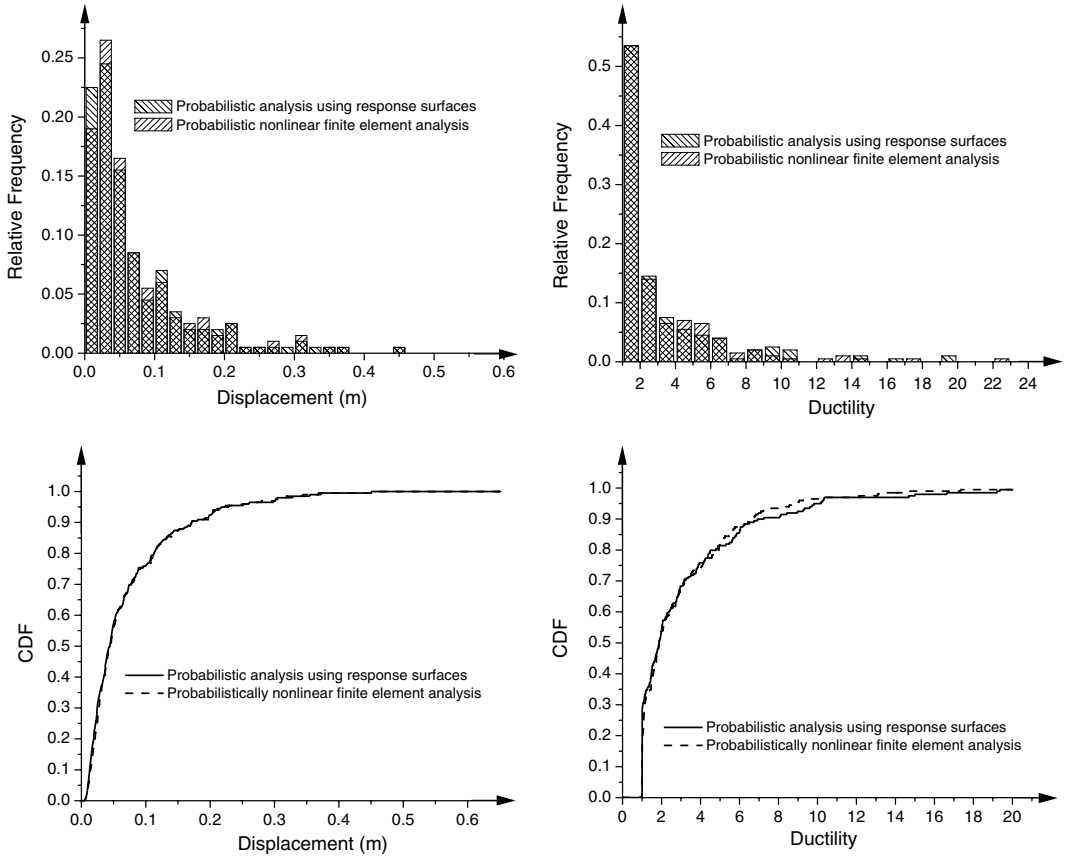

Fig. 13. Probabilistic results of the simply supported RC member (Example I).

According to Eqs. (15) and (16), y_m^{rc} and μ^{rc} of the member under a blast loading can be estimated from the corresponding y_m^{eq} and μ^{eq}, which are computationally simple and straightforward. By converting the continuous member into an equivalent SDOF system [7], these parameters including equivalent mass (m), equivalent force (F_1), equivalent initial stiffness (k_e), equivalent ultimate strength (R_m), natural period (T), elastic displacement ($y_e^{eq} = R_m/k_e$), and elastic energy ($E_{el} = ky_e^2/2$) can be obtained. Accordingly, y_m^{eq} and μ^{eq} are effortlessly solved with

$$y_m^{eq} = \frac{E_{max}}{k_e y_e^{eq}} + \frac{y_e^{eq}}{2} \quad \text{and} \quad \mu^{eq} = \frac{y_m^{eq}}{y_e^{eq}} \tag{17}$$

where E_{max} is computed with the non-dimensional energy factor ($C = E_{max}/E_{el}$) found from the energy spectra according to the ratios t_d/T and F_1/R_m [13]. The combination of Eqs. (15)–(17) with the probabilistic methods such as the Monte-Carlo simulation provides a simpler probabilistic solution for y_m^{rc} and μ^{rc} of RC flexural members in blast conditions taking different uncertainties into account.

However, it should be pointed out that unlike the situation where the responses of y_m^{rc} and μ^{rc} can be more accurately determined through nonlinear finite element analysis, Eqs. (15) and (16) only provide an approximate way to predict y_m^{rc} and μ^{rc} from the respective y_m^{eq} and μ^{eq} since e_y and e_μ are two uncertain nominal random variables following normal distribution. Considering the random effects of e_y and e_μ, the coefficients of variation (COV) for y_m^{rc} and μ^{rc} are obtained as

$$\mathrm{COV}(y_m^{rc}) = \frac{\sigma_{e_y}}{1 - f(\rho, SC)} \tag{18}$$

$$\mathrm{COV}(\mu^{rc}) = \frac{\sigma_{e_\mu}}{1 - g(\rho, SC)} \tag{19}$$

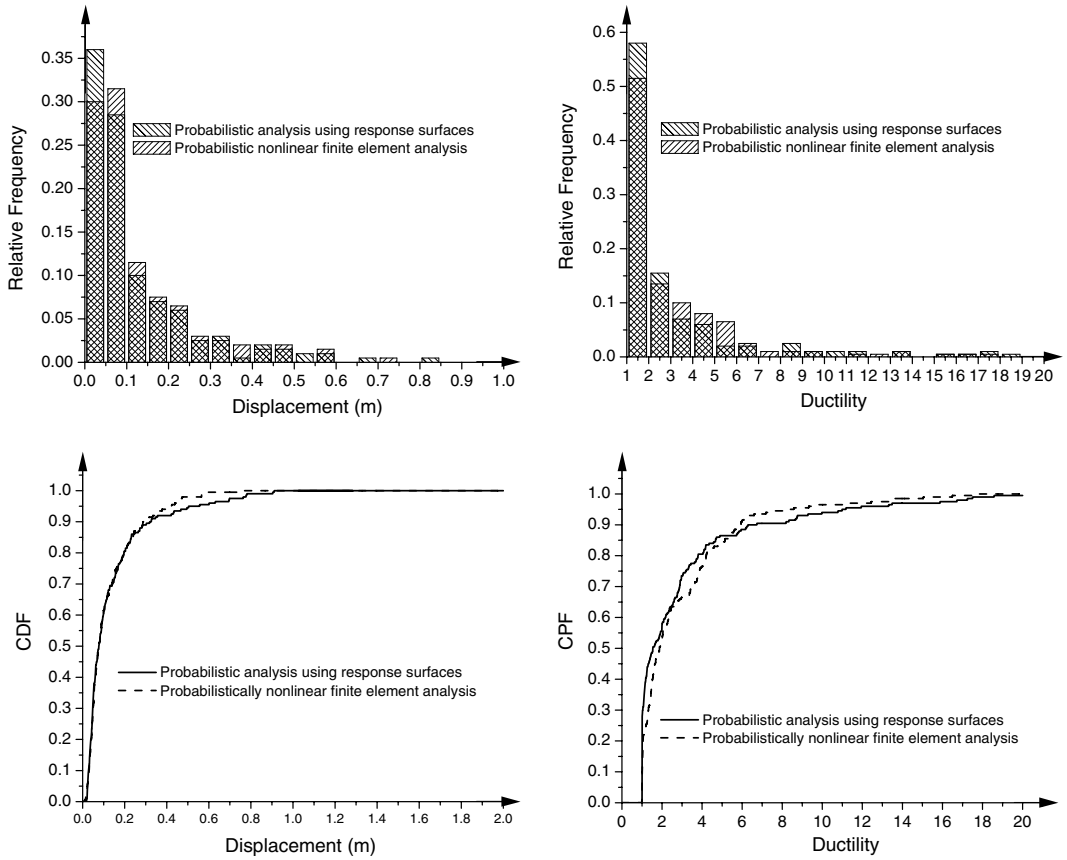

Fig. 14. Probabilistic results of the fixed/free RC member (Example II).

The COVs for y_m^{rc} and μ^{rc} have no relationship with their respective y_m^{eq} and μ^{eq} and they tend to change with ρ and support condition of the member as shown in Fig. 12. It is shown that the maximum COVs of y_m^{rc} for the simply supported, fixed/roller-supported and fixed/free members are generally less than 0.03, representing a significant concentration of y_m^{rc} around their mean values. The COVs of μ^{rc} for these types of members rang from 0.05 to 0.18 and rise gradually with the decline inρ. For the fixed/fixed members, the predicted y_m^{rc} is also concentrated around its mean values with the maximum COV less than 0.08, however, the μ^{rc} predicted from Eq. (16) has some deviation when ρ is less than 1.0%.

4. Numerical illustration and verification

For illustration, y_m^{rc} and μ^{rc} of four RC flexural members with different support conditions, whose details are shown in Table 5, are probabilistically evaluated using response surface with Eqs. (15) and (16) together with Monte-Carlo simulation [14]. The verifications of numerical results obtained are further performed as compared to the probabilistically nonlinear finite element analytical outcomes.

The uncertainties of different variables including f_{ds}, f_{dc}, E_s, E_c, A_s, d, and l are considered in the probabilistic response assessment of these members. Their means values are taken as those employed in Table 5 while their COVs are listed in Table 6 [15–17]. The blast loading brings out the most uncertainty to the structural responses. However, to date not enough information is available on the random properties of blast loadings applied to a structure in its lifetime. In this example it is assumed that W and R follows uniform distributions with the ranges as shown in Table 6. The parameters of e_y and e_μ are two additional independent random variables that link y_m^{rc} and μ^{rc} with the respective y_m^{eq} and μ^{eq}. Their distributions can be found in Fig. 11 with the zeros of mean values and the corresponding standard deviations at various support conditions.

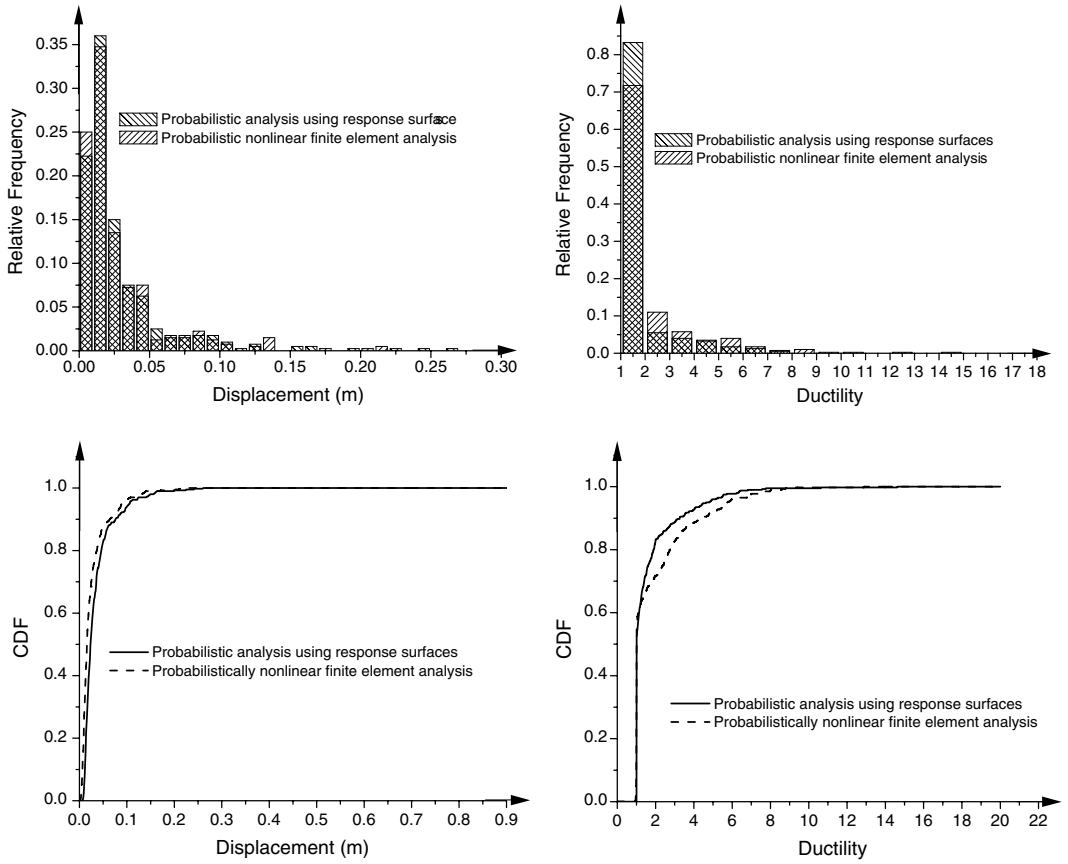

Fig. 15. Probabilistic results of the fixed/roller-supported RC member (Example III).

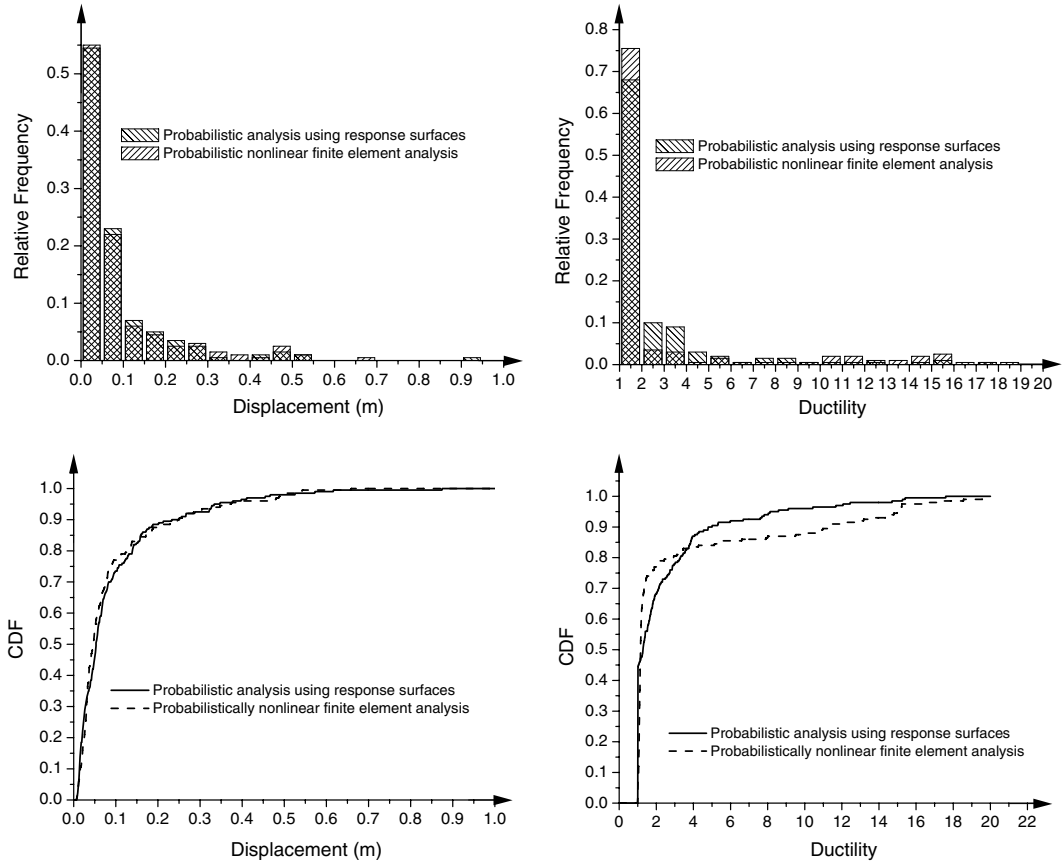

Fig. 16. Probabilistic results of the fixed/fixed RC member (Example IV).

The probabilistic response assessment of the four RC members involving the uncertainty of the above variables is accomplished through Monte-Carlo simulation. The choice of Monte-Carlo simulation for this situation is justified because the approach to predict y_m^{rc} and μ^{rc} using the response surface with Eqs. (15) and (16) is very simple. As a consequence, the simulation sample size can be selected relatively widely so as to achieve an accurate estimation without consuming much computational time and work. The probability density functions (PDFs) of y_m^{rc} and μ^{rc} for these concerned members and the corresponding cumulative distribution functions (CDFs) are computed and shown in Figs. 13–16. To verify the numerical results obtained, the probabilistic nonlinear finite element analyses of these examples are also performed and compared with the probabilistic analysis as shown in Figs. 13–16. Summarizing the results, it can be seen that the PDFs and CDFs of y_m^{rc} and μ^{rc} predicted using the response surface are in close agreement with those from the probabilistically nonlinear finite element analysis with the exception of μ^{rc} for the fixed/fixed member. The inconsistency in probabilistic distribution of μ^{rc} for the fixed/fixed member is mainly induced by the complicated resistance functions of fixed/fixed members. The CDFs of μ^{rc} predicted for the fixed/fixed member are on the conservative sides to some extent as compared to the probabilistically nonlinear finite element analysis.

5. Conclusions

A simple yet efficient approach of the probabilistic assessment of y_m^{rc} and μ^{rc} for RC flexural members under blast conditions is presented without carrying out probabilistically nonlinear finite element analysis. This approach is accomplished depending on the formulae of two indices (ς_y^{rc} and ς_μ^{rc}) that quantify the difference between the responses of RC members with those of equivalent SDOF systems.

The distribution of ς_y^{rc} and ς_μ^{rc} with different variables that have been selected randomly from their particular ranges within the blast-resistant design is generated through a large amount of numerical analyses. By comparing these distributions, it is found that the support condition and ρ have profound effects on ς_y^{rc} and ς_μ^{rc} while the variables other than support condition and ρ have some minor influences. To incorporate all variables effects, the formulae of ς_y^{rc} and ς_μ^{rc} are recommended including two items: a nonlinear fitting function correlated with ρ and support condition and a random variable (e_y and e_μ) to consider the influence of the others.

Computation of y_m^{rc} and μ^{rc} for RC flexural members under a blast loading becomes much simpler based on the formulae of ς_y^{rc} and ς_μ^{rc} since they can be easily derived from the corresponding y_m^{eq} and μ^{eq} that are computationally straightforward. By combining this approach with Monte-Carlo simulation, the probabilistic blast responses of RC members are conveniently evaluated accounting for different types of uncertainties. The PDFs and CDFs of y_m^{rc} and μ^{rc} obtained from ς_y^{rc} and ς_μ^{rc} have a good agreement with those from probabilistically nonlinear finite element analysis as indicated from numerical examples.

References

[1] ASCE Manual 42. Design of structures to resist nuclear weapons effects. American Society of Civil Engineers; 1985.
[2] Allgood JR, Swihart GR. Design of flexural members for static and blast loadings, ACI Monograph Series, No. 5; 1970.
[3] May GC, Smith PD. Blast effect on building: design of buildings to optimize resistance to blast loading. Thomas Telford; 1995.
[4] Bangash MYH. Impact and explosion: analysis and design. Oxford: Blackwell Scientific Publication; 1997.
[5] Chowdhury MR. Responses of beam structures due to blast loadings, PhD thesis, University of Cincinnati; 1987.
[6] Beshara BA. Nonlinear finite element analysis of RC structures subjected to blast loading, PhD thesis, City University, London; 1991.
[7] Biggs JM. Introduction to structural dynamic. New York: McGraw-Hill; 1964.
[8] Hilleborg A, Modeer M, Petersson PE. Analysis of crack formation and crack growth in concrete by means of fracture mechanics and finite elements. Cement Concrete Res 1976;6:773–82.
[9] Hyde DW. ConWep: weapons effects calculation program based on technique manual, TM5-855-1. United States Army Engineer Waterways Experiment Station; 1991.
[10] TM 5-855-1. Fundamental of protective design for conventional weapons. United States Department of the Army, Washington, DC; 1986.
[11] TM5-1300. Structures to resist the effects of accidental explosions, vol. IV, reinforced concrete design. United States Department of the Army; 1990.
[12] NFEC. Blast resistant structures. Naval Facilities Engineering Command, Design Manual 2.08, Alexandria, VA; 1986.
[13] Hai-Cheng Rong. Performance-based blast resistant design of reinforced concrete frame structures under distant explosions, PhD thesis, Nanyang Technological University; 2005.
[14] Kottegoda NT, Rosso R. Statistical, probability and reliability for civil and environmental engineers. New York: McGraw-Hill; 1996.
[15] Mirza SA, Hatzinikolas M, MacGregor JG. Statistical descriptions of strength of concrete. J Struct Eng ASCE 1979;105(6):1021–36.
[16] Mirza SA, MacGregor JG. Variations in dimensions of reinforced concrete members. J Struct Eng ASCE 1979;105(4):751–65.
[17] Val VD, Bljuger F, Yankelevsky DZ. Reliability assessment of damaged RC famed structures. J Struct Eng ASCE 1997;123(7):889–95.
[18] ABAQUS. ABAQUS/Standard User's Manual. HKS, Inc.; 2004.
[19] CEB-FIP Model Code 1990, Design Code. Thomas Telford, Switzerland; 1993.
[20] Malvar LJ, Crawford JE. Dynamic increase factors for concrete. In: Twenty-eighth DDESB seminar, Orlando, FL; 1998.
[21] Malvar LJ, Crawford JE. Dynamic increase factors for steel reinforcing bar. In: Twenty-eighth DDESB seminar, Orlando, FL; 1998.
[22] Seabold RH. Dynamic shear strength of reinforced concrete beams, part II. Naval Civil Engineering Laboratory, Port Hueneme, California; 1967.